Assessment of mitogen-activated protein kinases as therapeutic targets for the treatment of babesiosis and theileriosis

Özal MUTLU*

Biology Department, Faculty of Arts and Sciences, Marmara University, İstanbul, Turkey

Abstract: The Piroplasmida order comprises parasitic protozoa including the *Theileria* and *Babesia* species that are transmitted by vector ticks and can cause severe diseases in domestic and wild animals. Because of limited therapies and available drug resistance, the discovery of new, effective, and safer drugs for veterinary use is important. Mitogen-activated protein kinases (MAPK) are a group of serine-threonine protein kinases found in diverse species, including animals and protozoa that conduct vital cellular functions. Therefore, they have been at the centre of drug design studies for many years. Computer-aided structure-based drug design is a fast and effective way in drug discovery efforts to identify candidate compounds. In this study, we conducted comparative sequence analysis of MAPK proteins from the *Theileria* (*T. annulata, T. parva., T. orientalis,* and *T. equi*) and *Babesia* species (*B. bigemina, B. microti,* and *B. bovis*). Three-dimensional protein structures from relevant species (*T. annulata* and *B. bovis)* were modelled and compounds were screened for interaction. Results showed that the inhibitors designed for human use could also be potent against Prioplasmida MAPKs. Furthermore, the structural differences between Prioplasmida and mammalian MAPKs could be a way for researchers to better instigate selective drug design.

Key words: Mitogen-activated protein kinase, computer-aided drug design, theileriosis, babesiosis

1. Introduction

The *Theileria* and *Babesia* species (Order Piroplasmida) are unicellular protozoan parasites belonging to the phylum Apicomplexa that exhibit characteristic apical complex and apicoplast organelles. Apicomplexans are responsible for serious diseases such as toxoplasmosis (*Toxoplasma gondii*) and malaria in humans (*Plasmodium falciparum*); furthermore, theileriosis and babesiosis, mainly found in in domestic and farm animals, account for many deaths, cause a decline in the quality of life, decrease efficiency, and cause economic losses. *Theileria parva* and *T. annulata* cause East Coast fever and Tropical theileriosis, respectively, and occur in a wide range of geographical regions, including Africa, southern Europe, and Asia. The *Babesia* species is spread across southern Europe, Africa, America, Asia, and Australia and infects buffaloes, deer, sheep, cattle, and also humans [1–3]. Due to its resistance to buparvaquone, a conventionally used drug to treat theileriosis, and because of limited therapies in bovine babesiosis because of drug residues in by-products (milk and meat) and toxicity, it is necessary to discover safer and more effective and medications [4–8].

The MAPK signalling cascade is essential and regulates numerous cellular functions in eukaryotes such as proliferation, differentiation, development, inflammation, cell death, and stress response. They are phosphorylated by upstream MAP4Ks, MAP3Ks, and MAPKKs and turn on specific MAPKs terminated by the phosphorylation of nuclear factors and other kinases as cytosolic targets [9]. The MAPK family is classified under the cell cycle associated kinase (CMGC) group, along with 7 other families, including cyclin-dependent kinases (CDK), glycogen synthase kinases (GSK), and Cdk-like kinases (CLK) in humans [10].

Piroplasms have the smallest protein kinome size (there are only 42 protein kinases in *T. annulata*) compared to other organisms in Apicomplexa [11,12]. MAPK family proteins are presented in low numbers in all apicomplexans and found in only 2 members: *Theileria* and *Babesia* [11,13]. The absence of the entire STE group of serine/threonine protein kinases, joined to the MAPK signalling cascade in most eukaryotes, point to a unique signalling mechanism for apicomplexans [11]. There are many studies indicating the various roles of the MAPKs of protozoan parasites, some of which include ERK1

* Correspondence: ozal.mutlu@marmara.edu.tr

and ERK2 of *Giardia* spp. in encystation [14], MAPK2s of *P. falciparum* and *P. berghei* in the asexual cell cycle [15], and male gametocide formation [16], respectively. Moreover, various cellular functions in the *Leishmania* and *Trypanosoma* species have been reported, such as drug resistance, survival, proliferation, flagellum length control, and differentiation [17–20]. Along with other protein kinases, the MAPKs of protozoans are therefore attractive drug targets for the treatment of animal diseases [21,22].

Like other closely related apicomplexans, piroplasms have MAPKs like ERK7/8 (MAPK-15), designated as MAPK1 (MAPK2 in *T. gondii*), which carry a T(D) Y motif conserved in the activation loop [11,13,22]. However, the other MAPK, called MAPK2 (MAPK3 in *T. gondii*), is classified as an atypical MAPK with a TGH motif in the activation loop of *T. gondii* and piroplasms (TSH in *P. falciparum*) [13,21,22]. Their unique structural and functional features, compared to their mammalian counterparts and their evolutionary distance, make apicomplexan MAPKs attractive, druggable proteins, and this paves the way for selective drug design [13,21,23].

The main aim of this study is to repurpose the validated MAPK inhibitors, which were previously designed to combat human diseases on *Theileria* and *Babesia* MAP kinase 1 and 2 by computational structural biology approaches. This is the first report consisting of genome-wide screening of MAPK genes of piroplasms in detail with structural modelling, molecular dynamics analysis, and docking on *Theileria* and *Babesia* MAPK1 and MAPK2 proteins.

2. Material and methods

2.1 Sequence retrieval and analysis
Mitogen-activated protein kinase 2 sequences from *T. annulata* (Ankara str.), *T. orientalis* (Shintoku str.), *T. parva* (Muguga str.), and *T. equi* (WA str.) were retrieved from the NCBI RefSeq database. Sequences belonging to MAPK1s from both the *Theileria* and *Babesia* species [*B. bigemina, B. microti* (RI str.), and *B. bovis* (T2Bo str.)] and the MAPK2 of the *Babesia* species were predicted by DELTA-BLAST from NCBI (blast.ncbi.nlm.nih.gov) and BLASTP from the Ensembl Protist genome database (http://protists.ensembl. org) using *P. falciparum* 3D7 MAPK1 (XP_001348468.1) and MAPK2 (XP_001347818.1) as reference protein sequences. Resultant sequences were further confirmed by the Conserved Domain Database (CDD) from NCBI [24] and Pfam (protein families database) 32.0 [25] for an exact MAP kinase domain explication. Homologous sequences of MAPK1 and MAPK2 from the host species *Homo sapiens* and *Bos taurus* and the other apicomplexans (*T. gondii* and *Cryptosporidium parvum)* were identified by BLASTP search against RefSeq database using an E-value threshold of 1×10^{-10}.

MAPK1 and MAPK2 sequences from the *Theileria* and *Babesia* species and *H. sapiens* MAPK15 (NP_620590.2), MAPK11 (NP_002742) and MAPK14 (NP_001306.1), *B. taurus* MAPK15 (NP_001039575.1), MAPK11 (NP_001073804.1) and MAPK14 (NP_001095644.1), *T. gondii* ERK7 (XP_018636795.1) and MAPK3 (XP_002369585.1), and *C. parvum* MAPK2 (XP_001388246.1) sequences were analysed for conserved residues and divergences by applying multiple sequence analysis using the T-COFFEE multiple sequence alignment program [26]. Multiple sequence alignments were visualized on an ESPript 3.0 server [27]. Pairwise sequence alignments were conducted using the EMBOSS-water tool [28]. Phylogenetic relationships of MAPKs among apicomplexans were assigned via MEGA7 software [29] using the neighbor-joining method employing 500 bootstrap replications. Motifs within MAPK sequences were predicted and analysed by a MEME (Multiple Em for Motif Elicitation) server in MEME suite 5.1.0 [30]. Predictions of disordered regions were conducted by applying a false positive rate of 5% using a PrDOS server [31].

2.2. Comparative modelling and validation
A comparative modelling of the MAPK1 and MAPK2 structures from *T. annulata* and *B. bovis* was conducted with a Modeller 9.16 program [32] using template PDB files identified by BLASTP search against the PDB database, pairwise sequence alignment, and MAPK amino acid sequences. After the modelling process, potential energy was minimized by applying 2000 and 1000 steps of steepest descent and conjugate gradient algorithm, respectively, using the AMBERff14SB force field from Chimera 1.10.2 program [33]. Minimized structures were validated by ERRAT [34], ProSA [35], ProQ [36], and RAMPAGE [37] servers to attain 3D-model quality. Superimpositions and RMSD calculations based on C-alpha traces between models and templates were done in PyMOL 2.2.0 (PyMOL Molecular Graphics System, Ver. 2.0 (Schrödinger, NY, USA). Druggability assessment of protein cavities was predicted by a DoGSiteScorer server [38].

2.3. Molecular dynamics simulations and docking
The molecular dynamics of the MAPK1 and MAPK2 proteins of *T. annulata* and *B. bovis* were assessed by all-atom molecular dynamics simulations by using the NAMD 2.9 program [39] and the CHARMM force field. Structures were prepared within a water box and analysed after the MD simulations in the VMD 1.9.3 program [40] for RMSD and RMSF values. Initially, the first 2500 steps of the total 5000 steps of energy minimisation were conducted, wherein, at first, the protein structures were fixed; following this, the whole system was allowed free movement. A simulated annealing was applied for the system so that the temperature would be fixed at 300K in

NVT conditions. The system was then equilibrated in an NPT (1-atm pressure and 300 K temperature) ensemble. Lastly, a final 50 ns of production md simulation was done in same NPT conditions with 2fs timesteps. MAPK inhibitors were searched for and downloaded in the proper file formats from the IUPHAR/BPS Guide to Pharmacology (http://www.guidetopharmacology. org). Inhibitor and protein structures were prepared by LigPrep (Schrödinger, NY, USA) and ProteinPrepWizard, respectively, in Maestro (Schrödinger, NY, USA) by applying the OPLS3 force field. ATP binding pockets of MAPK1 and MAPK2 were selected as the target site, and receptor grids were defined by the Receptor Grid Generation module from Glide (Schrödinger, NY, USA). In total, 38 MAPK inhibitors were docked to the active site of proteins by applying a 2-tier procedure, wherein, as a first step, 30% of the best ligands that were selected by Glide SP docking were analysed further by a Glide XP docking step (Schrödinger, NY, USA). The top 5 scoring ligands were further assessed for their MM-GBSA binding energies in Prime (Schrödinger, NY, USA).

3. Results and discussion

3.1. Sequence retrieval and analysis

Evolutionary analyses of MAPKs from apicomplexans including *T. annulata, T. parva*, and *B bovis* were reported by Talevich et al. [11,12]. MAPK sequences from other *Theileria* and *Babesia* species were identified in detail by DELTA-BLAST searches from both NCBI RefSeq and the Ensembl Protist genome databases (Table 1). Based on homology, the *Theileria* and *Babesia* species contain 2 types of mitogen-activated protein kinases like *P. falciparum,* to which MAPK1 is evolutionary related with the MAPK15-like (ERK7/8) (CDD number: cd07852) protein; MAPK2 constitutes the "Serine/Threonine Kinase, Mitogen-Activated Protein Kinase domain" (CDD identity cd07834) (Table 1) [11,21,22].

According to the sequence analysis, MAPK1s from both species have an N-terminal kinase domain with a mean sequence length of 342. However, in the MAPK2 kinase domain located at the C-terminus, the sequence varies in length (Figures 1–2). When comparing sequences of piroplasm MAPKs with *B. taurus* and *H. sapiens* MAP kinases, MAPK1 shows homology with the mammalian MAPK15 (ERK7/8), and p38 MAPK (like MAPK11, MAPK14) proteins present a higher identity match with the piroplasm MAPK2. In fact, based on local alignments of MAPK1s from *B. bovis* and *T. annulata* in humans and cattle, MAPK15 showed about 38% and 48% identity between MAPK specific domains, respectively. In contrast, a 32% identity was shown between mammalian MAPK11 and MAPK2s of both *B. bovis* and *T. annulata* based on conserved kinase domains. Percentage identities of MAPK1 and MAPK2 vary between species of *Theileria* and *Babesia*. The closest sequences were between *T. annulata* and *T. parva*, whose identities were calculated at about 70% and 86.5% for MAPK1 and MAPK2, respectively. Phylogenetic trees also indicate a close

Table 1. Mitogen-activated protein kinases from *Theileria* and *Babesia* genomes.

| Organism/strain	NCBI protein Name	Assigned as	NCBI Accession	Length	CDD Kinase Domain
Theileria annulata/ Ankara	Protein kinase	MAPK1	XP_954104	709	7-354
	MAPK2	MAPK2	XP_954376	642	193-624
Theileria orientalis/ Shintoku	Protein kinase	MAPK1	XP_009689510	789	7-365
	MAPK2	MAPK2	XP_009689160	620	158-602
Theileria parva/ Muguga	Serine/threonine protein kinase	MAPK1	XP_766199	677	7-351
	MAPK2	MAPK2	XP_765886	642	193-624
Theileria equi/ WA	Protein kinase domain containing protein	MAPK 1	XP_004833198	598	5-342
	MAPK2	MAPK2	XP_004829898	581	146-563
Babesia bigemina	MAPK	MAPK1	XP_012766705	502	5-342
	MAPK	MAPK2	XP_012767953	600	173-582
Babesia microti/ RI	Extracellular signal-regulated kinase 2	MAPK1	XP_021338713	583	5-341
	MAPK	MAPK2	XP_012648003	556	106-537
Babesia bovis/ T2Bo	MAPK	MAPK1	XP_001610969	506	5-342
	MAPK	MAPK2	XP_001610481	584	159-566
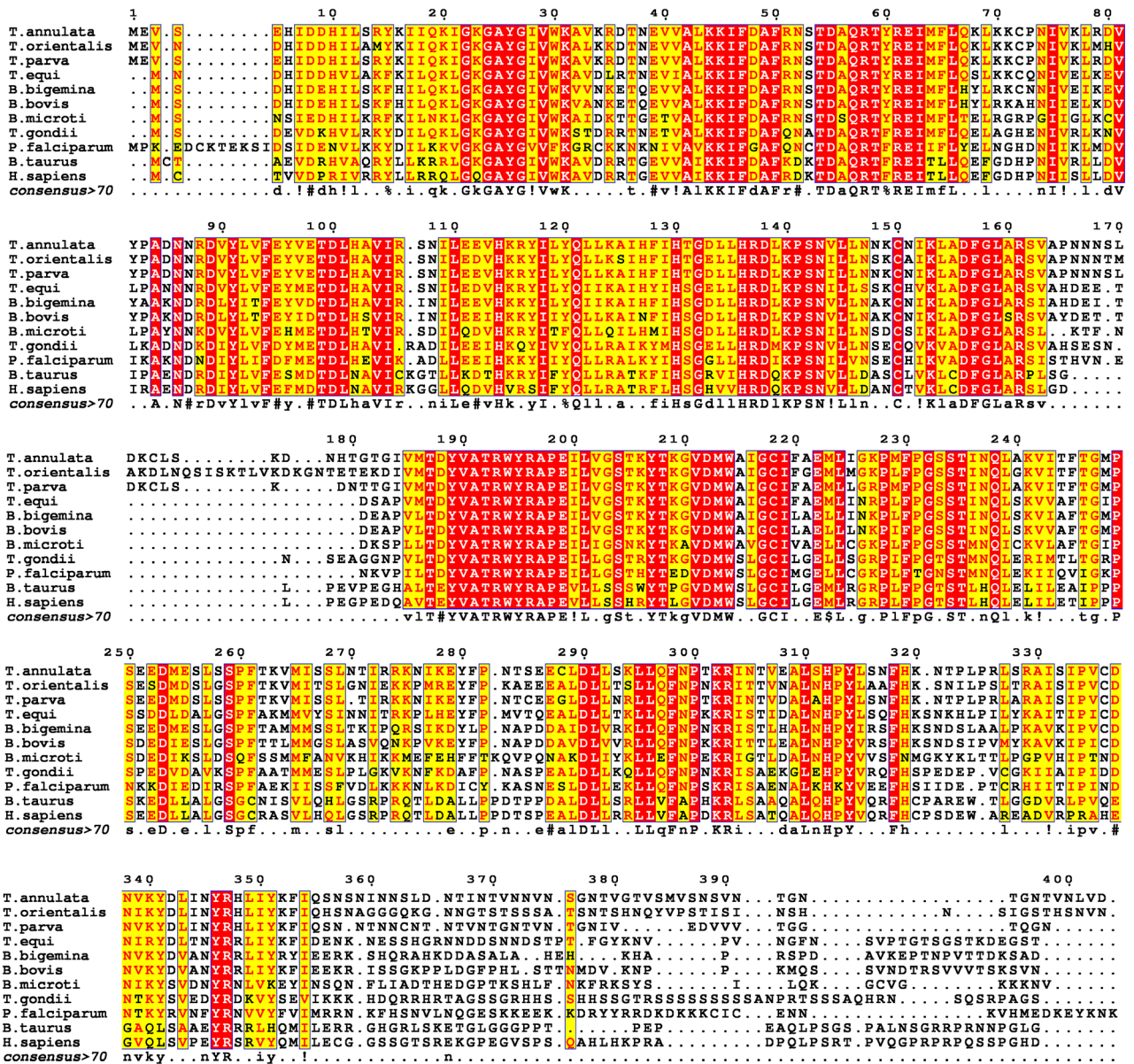
Figure 1. Multiple-sequence analysis of the MAPK1 proteins of piroplasms with *T. gondii* MAPK2, *P. falciparum* MAPK1, *B. taurus* MAPK15, and *H. sapiens* MAPK15 (based on 70% consensus).

relationship between apicomplexan MAPKs (Figures 3A and 3B). Both MAPK1 and MAPK2 have unstructured lengthy regions at their C and N-termini, respectively, and inside the activation loop segment like other MAP kinases from apicomplexans [21,22]. The multiple sequence alignment of the MAPK1s with those of other apicomplexans (*P. falciparum* and *T. gondii*) suggests a consensus on a phosphorylation lip triad located at the 186-TDY-190 position (*T. annulata* numbering), which designates the MAPK1 from the *Theileria* and *Babesia* species as a typical MAPK like that of *P. falciparum* (Figure 1) [22]. On the other hand, MAPK2s from the *Theileria* and *Babesia* species belong to atypical MAPKs, which bear a phosphorylation lip sequence in the form of a "TGH" motif, like the atypical MAPK of *T. gondii* (MAPK3) [13]. However, *B. microti* MAPK2 bears a triad motif, in the form of a "TSH", like the atypical *P. falciparum* MAPK2 (Figure 2) [21]. The MEME server was used to show motifs thought sequences (Figures 3C and 3D). Within MAPK1 proteins, there is a consensus across 8 motifs. However, 3 additional motifs were found in apicomplexan MAPK2 sequences, and 2 of them (7 and 8) were located at the C-terminus of the specific MAPK insertion site and not found in their mammalian counterparts. Since they have a
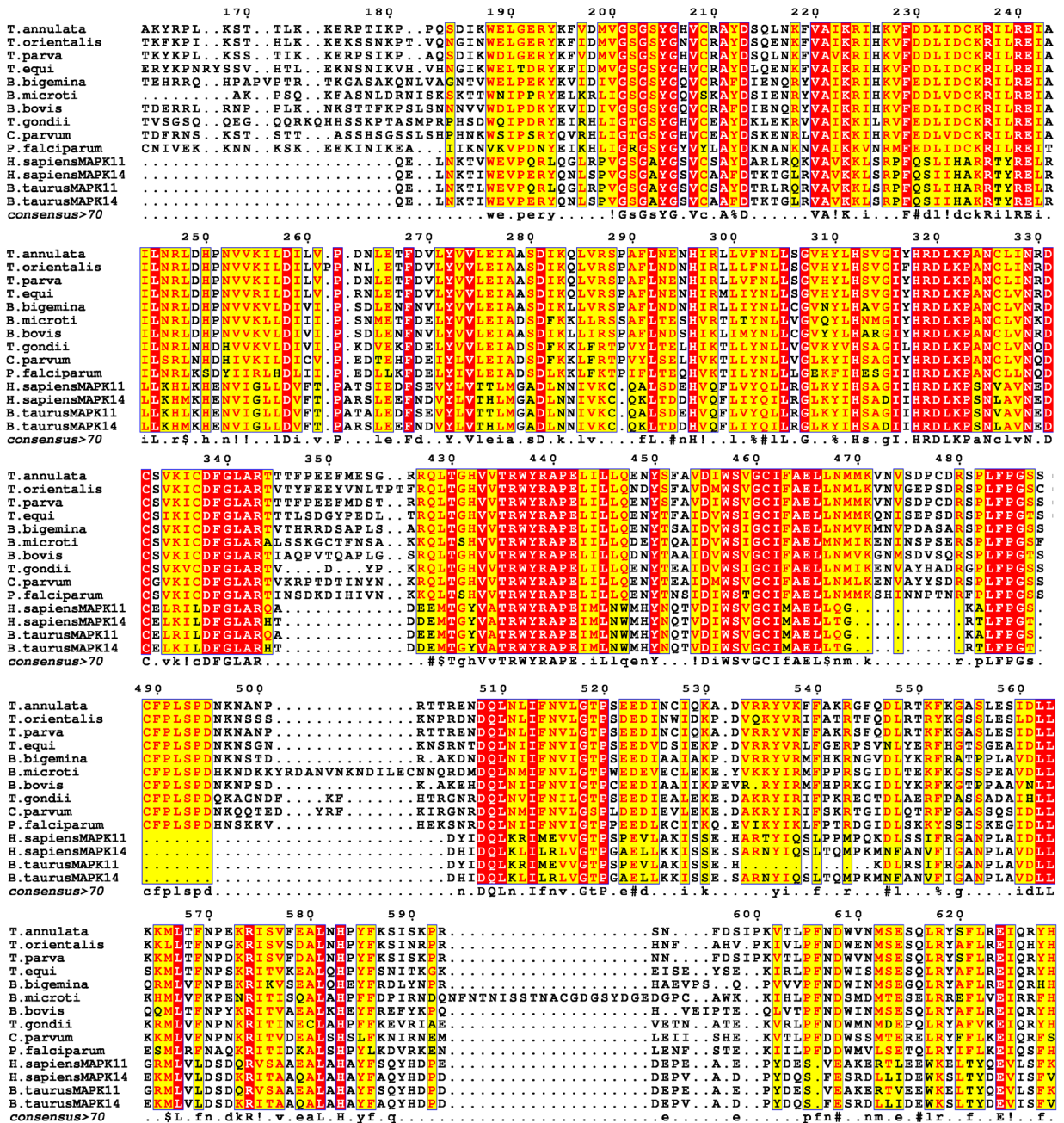
Figure 2. Multiple-sequence analysis of the MAPK2 proteins of piroplasms with *T. gondii* MAPK3, *P. falciparum* MAPK2, *C. parvum* MAPK2, *B. taurus* MAPK11 and MAPK14, *H. sapiens* MAPK11, and MAPK14 (based on 70% consensus).

role in the intrinsic autophosphorylation of a component of the MAPK insertion site of the mammalian p38-beta MAPK [41], additional motifs (7 and 8) in apicomplexans could be considered to be druggable sites for phylum-specific MAPK inhibitors (Figures 4A and 4B)

3.2. Comparative protein modelling and structure validation

Representative structures of the kinase domains of MAPK1 and MAPK2 from *T. annulata* and *B. bovis* were

modelled by a comparative approach using a Modeller 9.16 program based on the atomic coordinates of *C. parvum* MAPK1 (PDB ID: 3OZ6) and *T. gondii* MAPK3 (PDB ID: 3RP9) structures, respectively (Figure 4). MAPK1s from *T. annulata* and *B. bovis* show 56% (Query cover: 49% and E-value: 2e-142) and 52% (Query cover: 67% and E-value: 1e-137) identity matches with the crystal structure of *C. parvum* MAPK1. MAPK2 shows 49% (Query cover: 77% and E-value: 8e-173) and 57% (Query
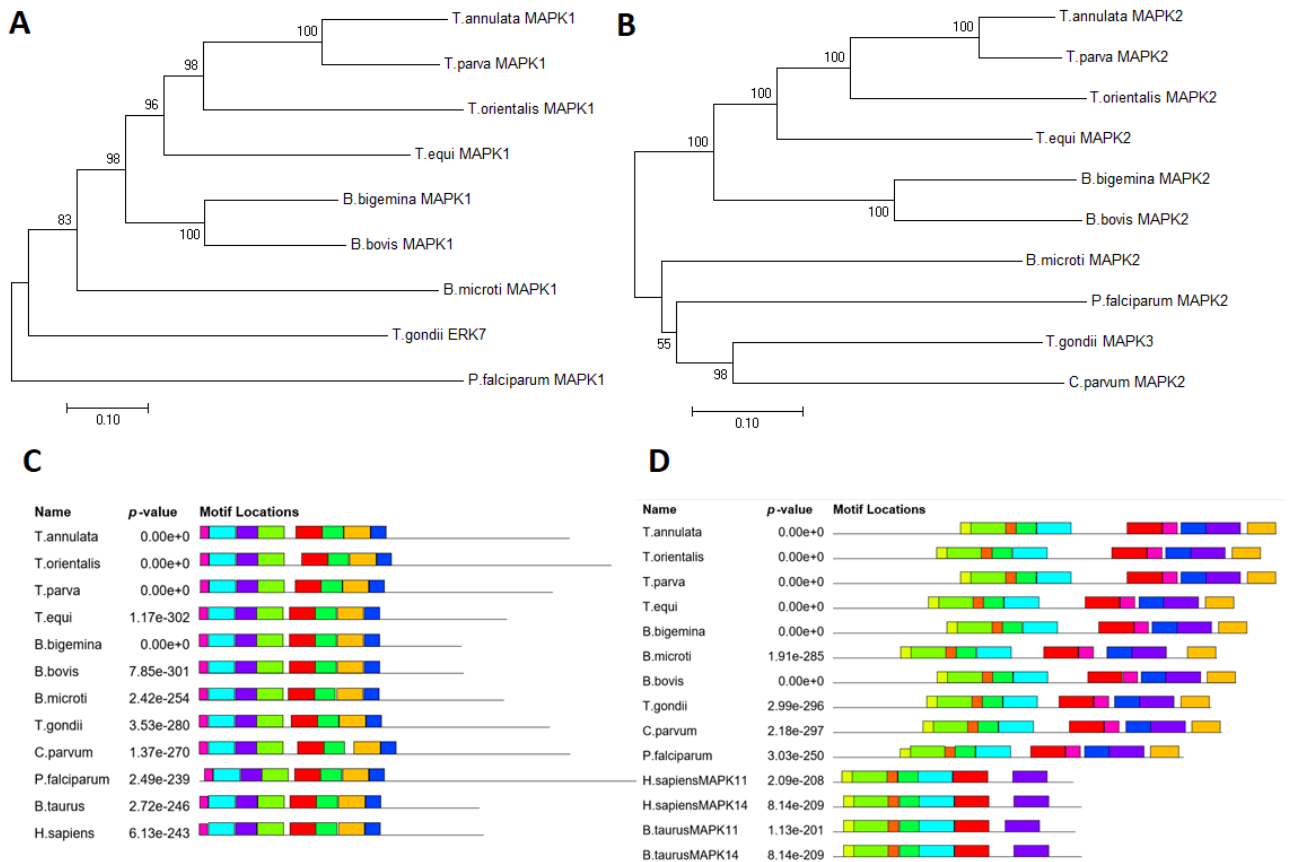
Figure 3. Phylogenetic relationships among apicomplexan MAPK1 (A) and MAPK2 (B) proteins. MEME motif analysis of MAPK1 from apicomplexans with *B. taurus* and *H. sapiens* MAPK15 (C) and MAPK2 with *B. taurus* and *H. sapiens* MAPK11 and MAPK14 (D).

cover: 72% and E-value: 4e-169) identity with the crystal structure of *T. gondii* MAPK3 for both *T. annulata* and *B. bovis*, respectively. Having a good sequence consensus is a crucial step for homology model predictions, and higher identity values make the construction of more accurate models possible. In this case, kinase domains were predicted based on templates, which have a mean identity of 54%, which is suitable for structure-based drug design and prediction of binding modes of small molecules in the active site. All generated models were subjected to geometry optimisation via potential energy minimisation. Resultant protein structures were further validated for 3D structure quality, and all structures were shown to have an adequate grade for further structural studies (Table 2).

Root mean square deviation (RMSD) values that represent structural similarities to template structures were found to be 0.697 Å and 0.684 Å for MAPK1s, 0.714 Å and 0.719 Å for MAPK2s for both *T. annulata* and *B. bovis*, respectively. These values are higher than expected due to the presence of long disordered activation loops in all structures. The ATP binding pocket is the major drug-targeting site, which has been the subject of many structure-

based drug design efforts [42]. DoGSiteScorer was used to predict targeting pockets and determine their drugabilities on MAPK1 and MAPK2 proteins. The server analysis results showed that the ATP sites have the highest scoring sites on MAPK structures for drug targeting (Table 2).

3.3. Molecular dynamics simulations and docking

Molecular dynamics of the *T. annulata* and *B. bovis* MAPK 1 and 2 were analysed by all-atom molecular dynamics simulations under NPT (1-atm pressure and 300 K temperature) conditions for 50 ns. Due to the absence of any molecular dynamics studies on apicomplexan MAPKs, structural features were compared with mammalian MAPK counterparts in this study [42,43]. As seen in Figure 5A, the MAPK1 structures of both *B. bovis* and *T. annulata* were found to be more stable than MAPK2 proteins, with average RMSD values of 3.05 Å and 3.78 Å, respectively. The highest RMSD value belongs to the *B. bovis* MAPK2, which is unstable and shows large fluctuations until the 40-ns mark. The disordered activation loop in MAPK2 is longer than that of MAPK1 proteins. Therefore, fluctuations due to this unstructured activation loop, especially in BbMAPK2, have been clearly
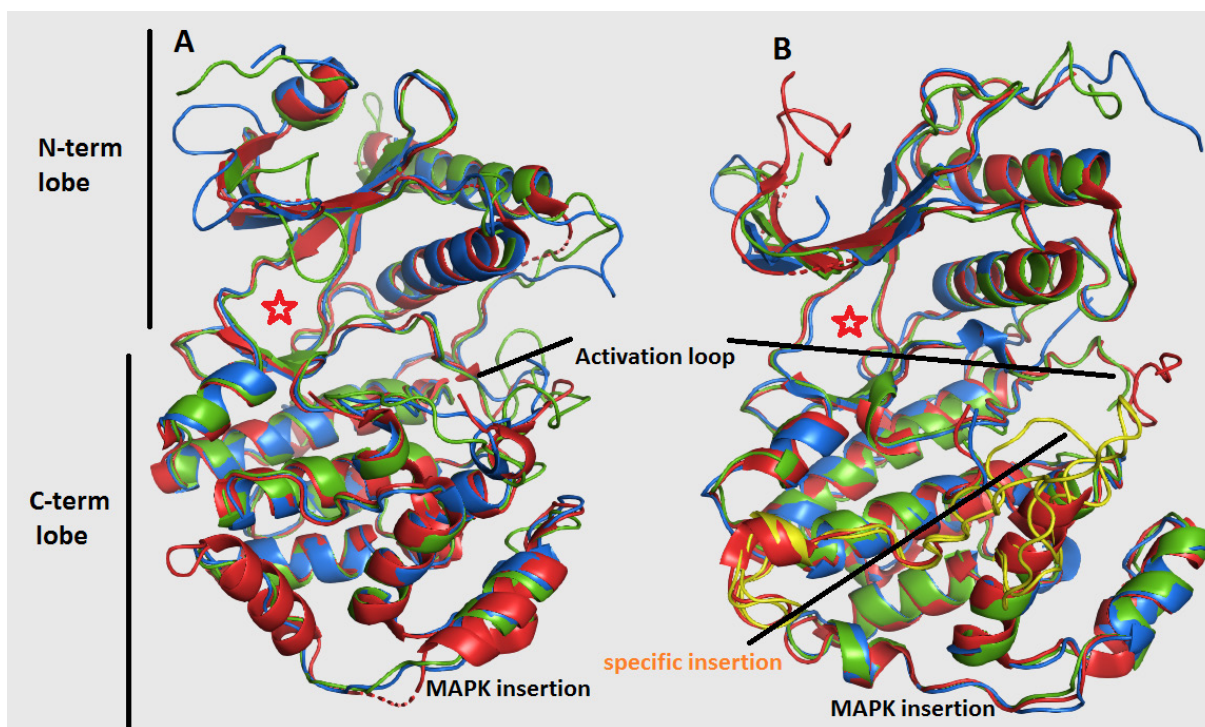
Figure 4. Cartoon view of the superimposition of MAPK1 (A) and MAPK2 (B) structures with template proteins of *C. parvum* (3OZ6_A) and *T. gondii* (3RP9_A). Red: templates; Green: *T. annulata* MAPK1 and MAPK2; Blue: *B. bovis* MAPK1 and MAPK2; specific insertions in piroplasm MAPK2 proteins are coloured yellow. A red asterisk shows ATP binding pockets used for the molecular docking site.

Table 2. Structural validations of MAPK kinase models.

	TaMAPK1	TaMAPK2	BbMAPK1	BbMAPK2
ProSA (Z-Score)	−7.87	−7.47	−7.66	−7.98
ProQ (LGScore)*	5.336	4.518	6.019	4.009
ERRAT overall score	93.0556	80.5419	87.7246	78.5714
Ramachandran plot scores				
Favoured region	87.2%	86.6%	88.4%	85.6%
Allowed region	12.0%	11.8%	9.3%	13.2%
Outlier region	0.8%	1.6%	2.3%	1.2%
RMSD**	0.697	0.714	0.684	0.719
DoGSiteScorer DrugScore	0.69	0.82	0.83	0.81

*LGscore > 1.5 = fairly good model; LGscore > 2.5 = very good model; LGscore > 4 = extremely good model.
**RMSD values were calculated for C-alpha traces by superimposing them with template PDB files.

observed on the RMSF graph between 145–193 amino acids (Figure 5B, red arrow).

In all MAPKs analysed in this study, large fluctuations in the activation loop were visible (Figure 5B, red arrow), and similar results have also been found regarding the activation loop thermal mobility in research conducted on the human p38 MAPK [42,43]. Another feature of RMSF analysis is the MAPK-specific insertion mobility in TaMAPK1 and BbMAPK1, which was also seen in the ERK2 and p38 MAPK (Figure 5B, green arrow) [43].
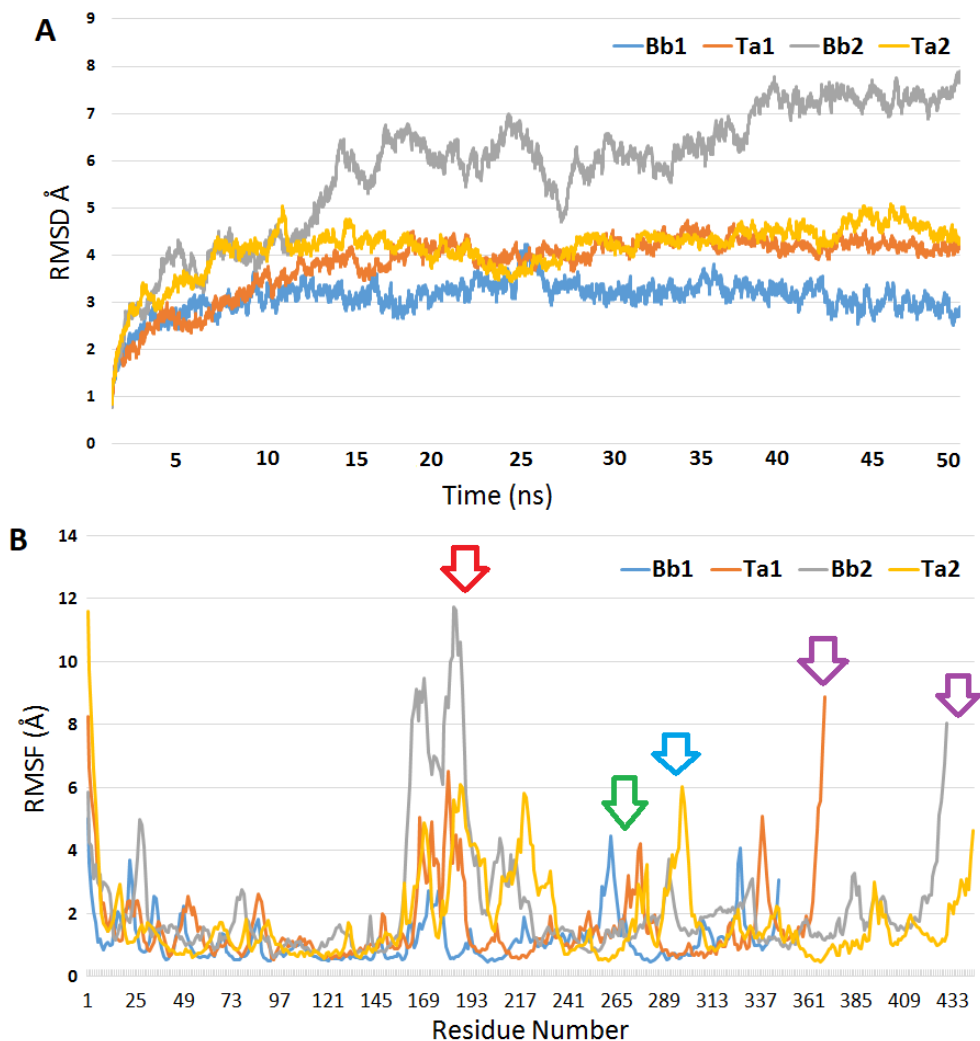
Figure 5. Root mean square deviation (RMSD) (A) and root mean square fluctuation (RMSF) (B) graphs of TaMAPK1 (orange), TaMAPK2 (yellow), BbMAPK1 (blue), and BbMAPK2 (grey) structures. Red arrow: activation loop; green arrow: MAPK specific insertion; blue arrow: specific insertion site; purple arrow: C-terminal region.

However, in the case of MAPK2s, the MAPK-specific insertion site did not show distinct fluctuations, unlike their mammalian counterparts, while the apicomplexan-specific insertion site shows a high degree of mobility (Figure 5B, blue arrow). Moreover, the C-tail region, like those of other MAPKs, showed higher fluctuations which are thought to have a role in allosteric regulations in MAP kinases [42–44]. By using the IUPHAR/BPS Guide to Pharmacology database, we identified 38 active MAPK kinase (especially p38 MAPK) inhibitors with the lowest IC50 values and screened MAPK targets via a 2-tier protocol consisting of the selection of the top 30% best compounds by SP docking and further analysis through a Glide XP docking step for the best possible hits (Table 3). Based on screening and molecular docking results, a compound with the PubChem ID 11714580

(named as PF-03715455) was found in all MAPKs' ATP binding sites, 3 of which (except TaMAPK2) had the highest DeltaG-binding energy. Pose views showed that the compound of interest interacted with binding pocket residues and made hydrogen bonds with TaMAPK1 (Ser142, Gly27, and Asp156), BbMAPK1 (Asp98), and BbMAPK2 (Arg23, Ala92, and Asp133) (Figures 6A, 6B, and 6D). Furthermore, with TaMAPK2, the compound formed a pi and a salt-bridge interaction with Tyr6 and Lys24 residues, respectively (Figure 6C). Another pi interaction also occurred between the 3-chloro-4-hydroxyphenyl moiety of the compound and the His100 residue of BbMAPK1.

Compound 11714580 is an investigational, small chemical currently in phase I trials that belongs to the pyrazole class and was designed to combat asthma and

Table 3. Molecular docking results of the MAPK inhibitor library on TaMAPK1 and 2 and BbMAPK1 and 2.

Pubchem ID	Target name	XP GScore	XP HBond	MMGBSA dG Bind
	TaMAPK1			
11714580*		–7.501	–1.372	–49.01
156422		–7.498	–1.212	–49.01
25125014**		–7.211	–1.040	–41.27
176167		–6.866	–0.148	–35.81
644241		–6.533	–0.973	–45.93
	TaMAPK2			
5228		–5.728	–0.485	–29.40
11714580*		–5.410	–0.434	–11.24
25125014**		–5.012	–0.960	–21.74
11314340		–4.896	–0.645	–21.18
10297982		–4.379	–1.300	–27.17
	BbMAPK1			
11314340		–7.077	–1.981	–29.34
11714580*		–6.903	–1.134	–40.97
25125014**		–6.456	–1.440	–35.20
11485656		–5.316	–1.407	–40.28
10297982		–4.706	–0.665	–38.94
	BbMAPK2			
10297982		–6.458	–0.696	–39.52
11714580*		–5.436	–1.587	–60.59
25125014**		–5.298	–3.095	–14.49
176167		–4.893	–1.560	–32.92
103905584		–4.435	–1.126	–26.38

*Pubchem ID_11714580 and ** Pubchem ID_25125014 compounds were found in all MAPKs.

pulmonary diseases by inhibiting the p38-alpha MAPK kinase in humans. Functional and structural studies have shown that the compound bound to the ATP site of human p38-alfa MAPK with high affinity (K_D: 0.001 nM) and showed preclinical safety properties for human use [45]. The other compound which interacted with all MAP kinases, with binding scores worse than 11714580, is 25125014 (BS-194), a pyrazolo[1,5-a]pyrimidine derivative designed for cancer chemotherapy. It shows potency and selectivity on human cyclin-dependent protein kinases (1, 2, 7, and 9) and ERK8 (MAPK15) with a low IC50 value (0.33 uM) [46]. These 2 small molecules, which have potency on human MAPKs, have interacted with MAPK 1 and 2 in *T. annulata* and *B. bovis* in silico, so further in vitro studies should be done for a more precise inhibition potential unravelling. Furthermore, reports have shown that the inhibitors designed for human MAPKs (especially for p38) act on apicomplexan organisms, including *P. falciparum*,

by blocking replication in human erythrocytes, *Eimeria tenella*, kinetoplastid parasite *L. donovani*, *T. gondii*, and the microsporidian parasite *Encephalitozoon cuniculi* [47–50]. This indicates a great potential for human MAPK inhibitors as promising drugs to fight parasitic diseases and makes a way for an improvement to the current inhibitors with higher efficiency and safety.

Since the first oncogene was designated as a protein kinase in 1978, great efforts in drug discovery have been made on different types of protein kinases. In addition, 13 small chemicals targeting serine/threonine protein kinases were approved by the FDA for use on human diseases [51,52]. Due to the pathophysiological roles of MAP kinases in apicomplexans, they have become molecules of strong interest in drug development [22,47]. In this study, we investigated the interaction potencies of MAPK kinase inhibitors with *T. annulata* and *B. bovis* MAPK 1 and 2 protein structures by using integrated computational
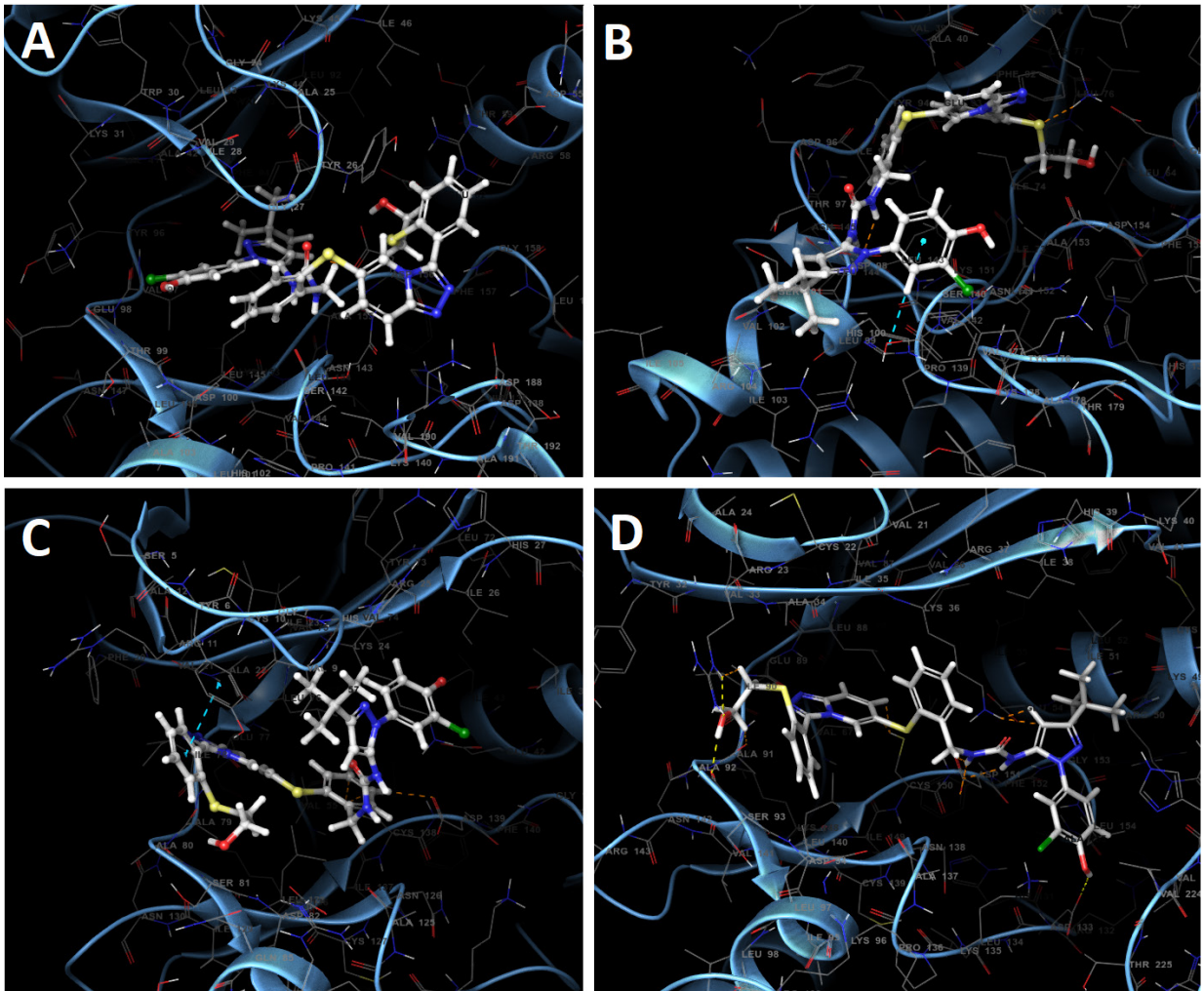
Figure 6. Molecular docking views of 11714580 (PubChem ID) within the ATP binding pocket of TaMAPK1 (A), BbMAPK1 (B), TaMAPK2 (C), and BbMAPK2 (D). Yellow and orange dots: H-bonds; cyan dots: pi interactions.

techniques. The results showed that the inhibitors designed for MAPKs of mammalians also have inhibition potency on piroplasm MAPKs. However, there is also an opportunity for selective drug design for piroplasm MAPKs, which show sequential and structural differences due to their evolutionary divergence when compared with their host counterparts.

Conflict of Interest
The author declares that there is no conflict of interest.

References

1. Bock R, Jackson L, de Vos A, Jorgensen W. Babesiosis of cattle. Parasitology 2004; 129 (Suppl): S247-269. doi: 10.1017/s0031182004005190

2. Bishop R, Musoke A, Morzaria S, Gardner M, Nene V. Theileria: intracellular protozoan parasites of wild and domestic ruminants transmitted by ixodid ticks. Parasitology 2004; 129 (Suppl): S271-283. doi 10.1017/s0031182003004748

3. Rashid M, Akbar H, Rashid I, Saeed K, Ahmad L et al. Economic significance of tropical theileriosis ona holstein friesian dairy farm in Pakistan. Journal of Parasitology 2018; 104 (3): 310-312. doi: 10.1645/16-179

4. Chatanga E, Mosssad E, Abubaker HA, Alnour SA, Katakura K et al. Evidence of multiple point mutations in *Theileria annulata* cytochrome b gene incriminated in buparvaquone treatment failure. Acta Tropica 2019; 191: 128-132. doi: 10.1016/j.actatropica.2018.12.041

5. Suarez CE, Alzan HF, Silva MG, Rathinasamy V, Poole WA et al. Unravelling the cellular and molecular pathogenesis of bovine babesiosis: is the sky the limit? International Journal for Parasitology 2019; 49 (2): 183-197. doi:10.1016/j.ijpara.2018.11.002

6. Mhadhbi M, Naouach A, Boumiza A, Chaabani MF, BenAbderazzak S et al. *In vivo* evidence for the resistance of *Theileria annulata* to buparvaquone. V*eterinary Parasitology* 2010; 169: 241-247. doi: 10.1016/j.vetpar.2010.01.013

7. Sharifiyazdi H, Namazi F, Oryan A, Shahriari R, Razavi M. Point mutations in the *Theileria annulata* cytochrome b gene is associated with buparvaquone treatment failure. V*eterinary Parasitology* 2012; 187: 431-435. doi: 10.1016/j.vetpar.2012.01.016

8. Mosqueda J, Olvera-Ramirez A, Aguilar-Tipacamu G, Canto GJ. Current advances in detection and treatment of babesiosis. Current Medicinal Chemistry 2012; 19 (10): 1504-1518. doi: 10.2174/092986712799828355

9. Plotnikov A, Zehorai E, Procaccia S, Seger R. The MAPK cascades: signaling components, nuclear roles and mechanisms of nuclear translocation. Biochimica et Biophysica Acta 2011; 1813 (9): 1619-1633. doi: 10.1016/j.bbamcr.2010.12.012

10. Manning G, Whyte DB, Martinez R, Hunter T, Sudarsanam S. The protein kinase complement of the human genome. Science 2002; 298 (5600): 1912-1934. doi: 10.1126/science.1075762

11. Talevich E, Mirza A, Kannan N. Structural and evolutionary divergence of eukaryotic protein kinases in Apicomplexa. BMC Evolutionary Biology 2011; 11: 321. doi: 10.1186/1471-2148-11-321

12. Talevich E, Tobin AB, Kannan N, Doerig C. An evolutionary perspective on the kinome of malaria parasites. Philosophical transactions of the Royal Society of London. Series B, Biological Sciences 2012; 367 (1602): 2607-2618. doi: 10.1098/rstb.2012.0014

13. Lacey MR, Brumlik MJ, Yenni RE, Burow ME, Curiel TJ. *Toxoplasma gondii* expresses two mitogen-activated protein kinase genes that represent distinct protozoan subfamilies. Journal of Molecular Evolution 2007; 64 (1): 4-14. doi:10.1007/s00239-005-0197-x

14. Argüello-Garciá R, Bazán-Tejeda ML, Ortega-Pierres G. Encystation commitment in Giardia duodenals: a long and winding road. Parasite 2009; 16 (4): 247-258. doi: 10.1051/parasite/2009164247

15. Dorin-Semblat D, Quashie N, Halbert J, Sicard A, Doerig C et al. Functional characterization of both MAP kinases of the human malaria parasite Plasmodium falciparum by reverse genetics. Molecular Microbiology 2007; 65 (5): 1170-1180. doi: 10.1111/j.1365-2958.2007.05859.x

16. Rangarajan R, Bei AK, Jethwaney D, Maldonado P, Dorin, D et al. A mitogen-activated protein kinase regulates male gametogenesis and transmission of the malaria parasite Plasmodium berghei. EMBO Reports 2005; 6 (5): 464-469. doi: 10.1038/sj.embor.7400404

17. Wiese M. Leishmania MAP kinases-familiar proteins in an unusual context. *International Journal* for *Parasitology* 2007; 37 (10): 1053-62. doi: 10.1016/j.ijpara.2007.04.008

18. Erdmann M, Scholz A, Melzer IM, Schmetz C, Wiese M. Interacting protein kinases involved in the regulation of flagellar length. Molecular Biology of the Cell 2006; 17 (4): 2035-2045. doi: 10.1091/mbc.E05-10-0976

19. Bao Y, Weiss LM, Ma YF, Lisanti MP, Tanowitz HB et al. Molecular cloning and characterization of mitogen-activated protein kinase 2 in *Trypanosoma cruzi*. Cell Cycle 2010; 9 (14): 2888-2896. doi: 10.4161/cc.9.14.12372

20. Ashutosh, Garg M, Sundar S, Duncan R, Nakhasi HL et al. Downregulation of mitogen-activated protein kinase 1 of *Leishmania donovani* field isolates is associated with antimony resistance. Antimicrobial Agents and Chemotherapy 2012; 56 (1): 518-525. doi: 10.1128/AAC.00736-11

21. Dorin D, Alano P, Boccaccio I, Cicéron L, Doerig C et al. An atypical mitogen-activated protein kinase (MAPK) homologue expressed in gametocytes of the human malaria parasite *Plasmodium falciparum*. Identification of a MAPK signature. Journal of Biological *Chemistry* 1999; 274 (42): 29912-29920. doi: 10.1074/jbc.274.42.29912

22. Brumlik MJ, Pandeswara S, Ludwig SM, Murthy K, Curiel TJ. Parasite mitogen-activated protein kinases as drug discovery targets to treat human protozoan pathogens. Journal of Signal Transduction 2011; 2011: 971968. doi: 10.1155/2011/971968

23. Huang H, Ma YF, BaoY, Lee H, Lisanti MP et al. Molecular cloning and characterization of mitogen-activated protein kinase 2 in *Toxoplasma gondii*. Cell Cycle 2011; 10 (20): 3519-3526. doi:10.4161/cc.10.20.17791

24. Marchler-Bauer A, Bo Y, Han L, He J, Lanczycki CJ et al. CDD/SPARCLE: functional classification of proteins via subfamily domain architectures. Nucleic Acids Research 2017; 45 (D1): D200-D203. doi: 10.1093/nar/gkw1129

25. El-Gebali S, Mistry J, Bateman A, Eddy SR, Luciani et al. The Pfam protein families database in 2019. Nucleic Acids Research 2019; 47 (D1): D427-D432. doi: 10.1093/nar/gky995

26. Notredame C, Higgins DG, Heringa J. T-Coffee: a novel method for fast and accurate multiple sequence alignment. Journal of Molecular Biology 2000; 302 (1): 205-217. doi: 10.1006/jmbi.2000.4042

27. Robert X, Gouet, P. Deciphering key features in protein structures with the new ENDscript server. Nucleic Acids Research 2014; **42** (W1): W320-W324. doi: 10.1093/nar/gku316

28. Madeira F, Park YM, Lee J, Buso N, Gur T et al. The EMBL-EBI search and sequence analysis tools APIs in 2019. Nucleic Acids Research 2019; 47 (W1): W636-W641. doi: 10.1093/nar/gkz268

29. Kumar S, Stecher G, Tamura K. MEGA7: Molecular Evolutionary Genetics Analysis version 7.0 for bigger datasets. Molecular Biology and Evolution 2016; 33: 1870-1874. doi: 10.1093/molbev/msw054

30. Timothy LB, Elkan C. Fitting a mixture model by expectation maximization to discover motifs in biopolymers. In: *Proceedings of the Second International Conference on Intelligent Systems for Molecular Biology;* Menlo Park, California, USA; 1994. pp. 28-36.

31. Ishida T, Kinoshita K. PrDOS: prediction of disordered protein regions from amino acid sequence. Nucleic Acids Research 2007; 35: W460-W464. doi: 10.1093/nar/gkm363

32. Webb B. Sali A. Comparative protein structure modeling using MODELLER. Current Protocols in Bioinformatics 2016; 54: 5.6.1-5.6.37. doi: 10.1002/cpbi.3

33. Pettersen EF, Goddard TD, Huang GS, Couch DM, Greenblatt EC et al. UCSF Chimera-a visualization system for exploratory research and analysis. Journal of Computational Chemistry 2004; 25: 1605-1612. doi: 10.1002/jcc.20084

34. Colovos C, Yeates TO. Verification of protein structures: patterns of nonbonded atomic interactions. Protein Science 1993; 2 (9): 1511-1519. doi: 10.1002/pro.5560020916

35. Wiederstein M, Sippl MJ. ProSA-web: interactive web service for the recognition of errors in three-dimensional structures of proteins. Nucleic Acids Research 2007; 35: W407-W410. doi: 10.1093/nar/gkm290

36. Wallner B, Elofsson A. Can correct protein models be identified? Protein Science 2003; 12 (5): 1073-1086. doi: 10.1110/ps.0236803

37. Lovell SC, Davis IW, Arendall WB, de Baker PI. Structure validation by Cα geometry: φ, ψ and Cβ deviation. Proteins 2003; 50 (3): 437-450. doi: 10.1002/prot.10286

38. Volkamer A, Kuhn D, Grombacher D, Rippmann F, Rarey M. Combining global and local measures for structure-based druggability predictions. *Journal of Chemical Information* and *Modeling* 2012; 52: 360-372. doi: 10.1021/ci200454v

39. Phillips JC, Braun R, Wang W, Gumbart J, Tajkhorshid E. Scalable molecular dynamics with NAMD. Journal of Computational Chemistry 2005; 16 (16): 1781-1802. doi: 10.1002/jcc.20289

40. Humphrey W, Dalke A, Schulten K. VMD: visual molecular dynamics. Journal of *Molecular Graphics* 1996; 14 (1); 33-38. doi: 10.1016/0263-7855(96)00018-5.

41. Beenstock J. Ben-Yehuda S, Melamed D, Admon A, Livnah O et al. The p38 Mitogen-activated protein kinase possesses an intrinsic autophosphorylation activity, generated by a short region composed of the -G Helix and MAPK Insert. The Journal of Biological Chemistry 2014; 289 (34): 23546-23556. doi: 10.1074/jbc.M114.578237.

42. Yang L, Sun X, Ye Y, Lu Y, Zuo J et al. p38α mitogen-activated protein kinase is a druggable target in pancreatic adenocarcinoma. Frontiers in Oncology 2019; 9: 1294. doi: 10.3389/fonc.2019.01294.

43. Nguyen T, Ruan Z, Oruganty K, Kannan N. Co-conserved MAPK features couple D-domain docking groove to distal allosteric sites via the C-terminal flanking tail. PLoS One 2015; 10 (3): e0119636. doi: 10.1371/journal.pone.0119636.

44. Buschbeck M, Ullrich A. The unique C-terminal tail of the mitogen-activated protein kinase ERK5 regulates its activation and nuclear shuttling. Journal of Biological Chemistry 2005; 280 (4): 2659-2667. doi: 10.1074/jbc.M412599200.

45. Millan DS, Bunnage ME, Burrows JL, Butcher KJ, Dodd PG et al. Design and synthesis of inhaled p38 inhibitors for the treatment of chronic obstructive pulmonary disease. *Journal* of *Medicinal Chemistry* 2011; 54 (22): 7797-7814. doi: 10.1021/jm200677b.

46. Heathcote DA, Patel H, Kroll SH, Hazel P, Periyasamy M et al. A novel pyrazolo[1,5-a]pyrimidine is a potent inhibitor of cyclin-dependent protein kinases 1, 2, and 9, which demonstrates antitumor effects in human tumor xenografts following oral administration. *Journal* of *Medicinal Chemistry* 2010; 53 (24): 8508-8522. doi: 10.1021/jm100732t.

47. Brumlik MJ, Nkhoma S, Kious MJ, Thompson GR 3rd, Patterson TF et al. Human p38 mitogenactivated protein kinase inhibitor drugs inhibit *Plasmodim falciparum* replication. Experimental Parasitology 2011; 128 (2): 170-175. doi: 10.1016/j.exppara.2011.02.016

48. Bussière FI, Brossier F, Le Vern Y, Niepceron A, Silvestre A et al. Reduced parasite motility and micronemal protein secretion by a p38 MAPK inhibitor leads to a severe impairment of cell invasion by the apicomplexan parasite *Eimeria tenella*. PloS One 2015; 10 (2): e0116509. doi: 10.1371/journal.pone.0116509.

49. Kaur P, Garg M, Hombach-Barrigah A, Clos J, Goyal N. MAPK1 of *Leishmania donovani* interacts and phosphorylates HSP70 and HSP90 subunits of foldosome complex. Scientific Reports 2017; 7 (1): 10202. doi: 10.1038/s41598-017-09725-w.

50. Wei S, Daniel BJ, Brumlik MJ, Burow ME, Zou W et al. Drugs designed to inhibit human p38 mitogen-activated protein kinase activation treat *Toxoplasma gondii* and *Encephalitozoon cuniculi* infection. Antimicrobial Agents and Chemotherapy 2007; 51 (12): 4324-4328. doi: 10.1128/AAC.00680-07.

51. Cohen, P. Protein kinases-the major drug targets of the twenty-first century? Nature Reviews Drug Discovery 2002; 1: 309-315.

52. Roskoski R Jr. Properties of FDA-approved small molecule protein kinase inhibitors. Pharmacological Research 2019; 144: 19-50. doi: 10.1016/j.phrs.2019.03.006.